Environmental Pollution 265 (2020) 114969

Contents lists available at ScienceDirect

Environmental Pollution

journal homepage: www.elsevier.com/locate/envpol

Environmental and human health risks of arsenic in gold mining areas in the eastern Amazon☆

Hamilton Ferreira de Souza Neto [a], Wendel Valter da Silveira Pereira [a], Yan Nunes Dias [a], Edna Santos de Souza [b], Renato Alves Teixeira [b], Mauricio Willians de Lima [a], Silvio Junio Ramos [c], Cristine Bastos do Amarante [d], Antonio Rodrigues Fernandes [a], *

[a] *Federal Rural University of Amazon, Belém, PA, Brazil*
[b] *Federal University of Southern and Southeastern Pará, Marabá, PA, Brazil*
[c] *Vale Institute of Technology – Sustainable Development, Belém, PA, Brazil*
[d] *Emílio Goeldi Museum of Pará, Belém, PA, Brazil*

ARTICLE INFO

Article history:
Received 18 October 2019
Received in revised form
3 June 2020
Accepted 3 June 2020
Available online 9 June 2020

Keywords:
Risk assessment
Environmental pollution
Arsenic bioaccessibility
Arsenic fractionation
Arsenic contamination

ABSTRACT

Knowledge of arsenic (As) levels in gold (Au) mining areas in the Amazon is critical for determining environmental risks and the health of the local population, mainly because this region has the largest mineral potential in Brazil and one of the largest in the world. The objective of this study was to assess the environmental and human health risks of As in tailings from Au exploration in the eastern Amazon. Samples were collected from soils and tailings from different exploration forms from 25 points, and the total concentration, pollution indexes and human health risk were determined. Concentrations of As were very high in all exploration areas, especially in tailings, whose maximum value reached 10,000 mg kg^{-1}, far above the investigation value established by the Brazilian National Council of the Environment, characterizing a polluted area with high environmental risk. Exposure based on the daily intake of As demonstrated a high health risk for children and adults, whose non-carcinogenic risk indexes of 17.8, extremely above the acceptable limit (1.0) established by the United States Environmental Protection Agency. High levels of As in reactive fractions in underground, cyanidation, and colluvium mining areas, as well as extremely high gastric and intestinal bioaccessibility were found, suggesting that high levels may be absorbed by the local population. The results show that the study area is highly polluted through Au mining activities, putting the environment and population health at risk, and that there is an urgent need for intervention by the environmental control agencies for remediation.

1. Introduction

Arsenic (As) is considered the most hazardous and harmful element to human health (USEPA, 2001). The high toxicity of this metalloid to humans, plants, and animals, as well as increasing concentrations in soil and water, has raised growing concern about the contamination risk in many parts of the world (Minatel et al., 2018; Thouin et al., 2018). This element is widely distributed in the environment and may be released by weathering and anthropic actions. The most abundant inorganic forms of As in terrestrial and aquatic environments are arsenate (AsV) and arsenite (AsIII) (Bundschuh et al., 2013).

The average concentration of As in the soil is 6.83 mg kg^{-1} (Kabata-Pendias, 2010). In soils under natural vegetation areas without anthropic interference from the eastern Amazon, the mean concentration of As is 1.10 mg kg^{-1}, while the quality reference value (QRV) is 1.4 mg kg^{-1} (Fernandes et al., 2018). In China, the QRV is 5.2 (Chen et al., 1991) and in Spain it is 49.5 mg kg^{-1} (Martinez-lladó et al., 2008). In Denmark (soil quality criterion) and in the Netherlands (target value), the values adopted are 10 and 29 mg kg^{-1}, respectively (Zhou et al., 2017). Concentrations of As have increased and caused environmental contamination due to anthropic activities, such as mining (with emphasis on the processing of gold (Au) and base metals), use of arsenic pesticides, wood preservatives, energy generation, and inadequate disposal of household and industrial waste (Odumo et al., 2018; Wang and Mulligan, 2006).

☆ This paper has been recommended for acceptance by Jörg Rinklebe.
* Corresponding author.
E-mail address: antonio.fernandes@ufra.edu.br (A.R. Fernandes).

https://doi.org/10.1016/j.envpol.2020.114969
0269-7491/© 2020 Elsevier Ltd. All rights reserved.

In the majority of Au mines, As is the element that receives the most environmental concern. Contamination by As from mining activities is well documented in various parts of the world. In Minas Gerais, Brazil, high concentrations of As were observed in wastes from Au mining areas, especially in the open pit mine (Ono et al., 2012). In the Amazon, studies on contamination by potentially toxic elements (PTEs) have focused on mercury (Hg), mainly in artisanal Au mining areas (Castilhos et al., 2015; Faial et al., 2015). Although there are high concentrations of PTEs in Au mining wastes (Ono et al., 2012; Souza et al., 2017), few studies have been carried out on the levels of As in Au exploitation areas in the Amazon.

Artisanal mining is the exploration of marginal ore deposits which are not enough lucrative to large-scale mining. In most artisanal mining areas, which can be legal or illegal, rudimentary techniques have been used to explore Au (Zvarivadza, 2018). In the Amazon, artisanal and small-scale mining began in the last century and still occur in this region, mainly clandestinely and without environmental control, as in the Serra Pelada artisanal mine, where high metal concentrations contaminated the environment and caused population health risks (Pereira et al., 2020; Souza et al., 2017; Teixeira et al., 2019).

Exposure to As is considerably worrying due to the strong toxicity of this element for many human body organs (Chatterjee et al., 2018). In this sense, risk assessment in areas with high concentrations of As is extremely important, especially when considering not only the total concentration (Yusà et al., 2018) that may overestimate the risk, but also bioavailability, since only a fraction is bioavailable (Li et al., 2014). In this study, bioavailability was assessed through bioaccessibility, simulating digestive and/or respiratory processes (Coufalík et al., 2016; Huang et al., 2016; Mendoza et al., 2017; Pereira et al., 2020), as well as chemical fractionation as appropriate tools for decision-making regarding risk assessment (Ono et al., 2012).

Information on As concentrations and their risks to human health and environment in Au mining areas from the Amazon is essential for government decision-making on remediating and reduce health risks, which is mainly because this region has the greatest mineral potential in Brazil and one of the largest in the world (Souza et al., 2017). In this sense, the objective was to assess the risk of As contamination in the environment and the impact on human health from total and bioavailable concentrations in areas under different forms of Au mining.

2. Materials and methods

2.1. Study area

The study area is located in the municipality of Cachoeira do Piriá, northeastern Pará (Latitude: 1°44′33″ South, Longitude: 46°34′15″ West), Amazon region, northern Brazil. The municipality appeared on the banks of the artisanal mine during the 80s, covers 2462 km^2 and has approximately 30,000 inhabitants. The main economic activity is mineral exploration (Hinton and Veiga, 2009; IBGE, 2018). According to the classification proposed by Köppen and Geiger, the climate of the municipality is tropical monsoon, with annual mean temperature and average rainfall of 26 °C and 2300 mm, respectively, comprising a rainy period from December to May and a dry period from June to November, with a precipitation difference of 356 mm between the driest and the wettest months (INMET, 2018).

The entire area of the municipality is covered by the Cachoeira deposit, one of the main Au deposits of the Chega Tudo Formation of the Gurupi Belt (Mosher, 2013). This region has a complex lithologic constitution with alternating host rocks containing basalt, andesite, dacite, graphite, sericite, schist chlorite, chlorite-talc schist, silexist and microdiorite (Klein et al., 2017). It is associated with many mineral deposits, especially sulfide minerals, such as arsenopyrite. Given the exposure to atmosphere, these minerals can be worn and oxidized, releasing As and other PTEs (Murciego et al., 2011).

In Cachoeira do Piriá, mining was carried out by companies (legalized) and artisanal miners (not legalized) until 2013, in areas where Au is found at a depth of 40–150 m, in quartz veins, vein networks, and shear zones (Mosher, 2013; Santos, 2004). Currently, exploration is performed only by an artisanal cooperative through three main forms: i) underground mining (Fig. 1S) at a depth of approximately 150 m, where amalgamation is carried out with conduction of the leachate (solid material + water) in a copper plate containing Hg for retention of Au, whose tailings (considered in sampling) were deposited 13 and 7 years ago, occupying an area greater than 12 ha, ii) colluvial mining (Fig. 2S), where unconsolidated materials (usually sand/gravel, where Au is found) are extracted using a hydraulic pump and conducted through a wooden channel with carpet at the base, with amalgamation by mixing the material (retained on the carpet) with Hg in a container, followed by burning, generating tailings that occupy an area of approximately 20 ha, and iii) cyanidation mining (Fig. 3S), where wastes from underground exploration are reprocessed using alkaline cyanide solution for complexing residual Au, whose tailings extend for 3 ha. The extent of the areas was estimated using the ArciGis software. In addition to mining areas, the study site includes a natural forest, which was considered as a reference area.

The mining areas extend from the banks up to 1500 m away from the Macaco River. These mines are located in the Gurupi formation (Fig. 1), which comprises rocks from the metavolcanic sedimentary domain, defined by shear zones, hydrothermally altered and with less deformed internal portions that preserved the primary igneous textures (Ribeiro, 2002). The natural forest includes riparian vegetation of the Macaco River and is located approximately 5 km away from the mines, with similar lithology to the exploration areas, placed on the Piriá formation (Fig. 1), which includes Precambrian rocks of the Gurupi Belt and has undergone hydrothermal alterations, producing a relatively constant mineralogical composition of quartz, dolomite, albite and sulfide (predominantly pyrite and arsenopyrite) (Mosher, 2013). Both mining areas and natural forest belong to the Macaco River sub-basin (tributary of the Piriá River), which together with the Emboraí River, constitute the main rivers that form the Atlantic hydrographic basin – North/Northeast section (MMA, 2001; Cordeiro et al., 2017).

2.2. Sampling of soils and mining tailings

The sampling was performed in April 2018, considering only areas where collection was allowed by the artisanal miners (Table 1S). The areas were identified as: i) G1 - tailings from underground mining with 13 years of disposal; ii) G2 - tailings from underground mining with 7 years of disposal; iii) G3 - tailings from recent colluvial mining; and iv) G4 - tailings from recent cyanidation mining that reprocesses waste from underground mining. The native forest area not impacted by mining of Au (reference area) was identified as NF.

In each area, five composite samples equidistant 50 m from each other were collected, totaling 25 samples (Fig. 2). Each composite sample (about 2.5 kg) was composed of five subsamples (about 0.5 kg) collected in the 0.0–0.2 m layer, with a stainless-steel helical drill, in order to avoid sample contamination. The subsamples were placed in polyethylene bags and mixed. Each bag (containing

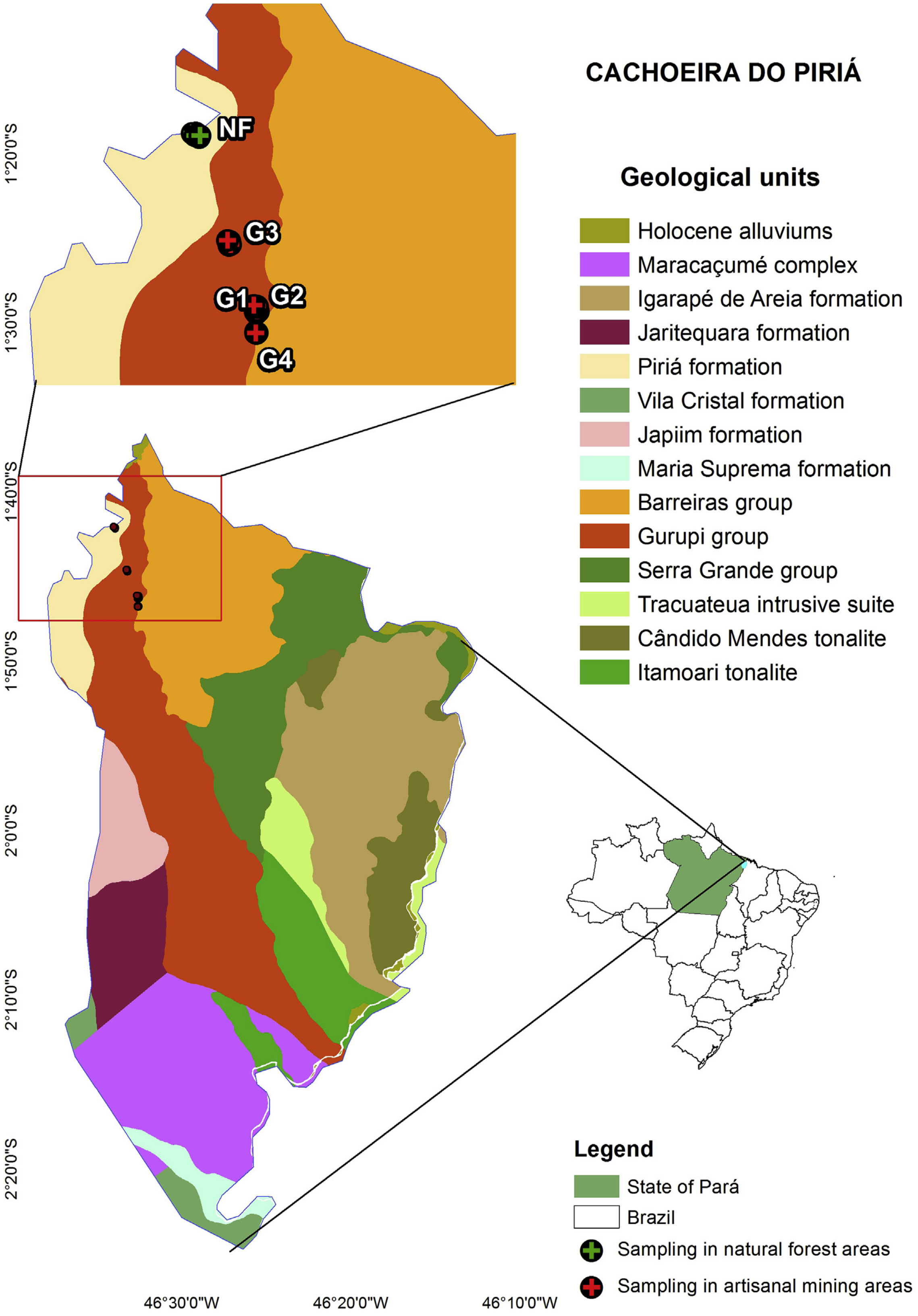

Fig. 1. Geological composition of the study area.

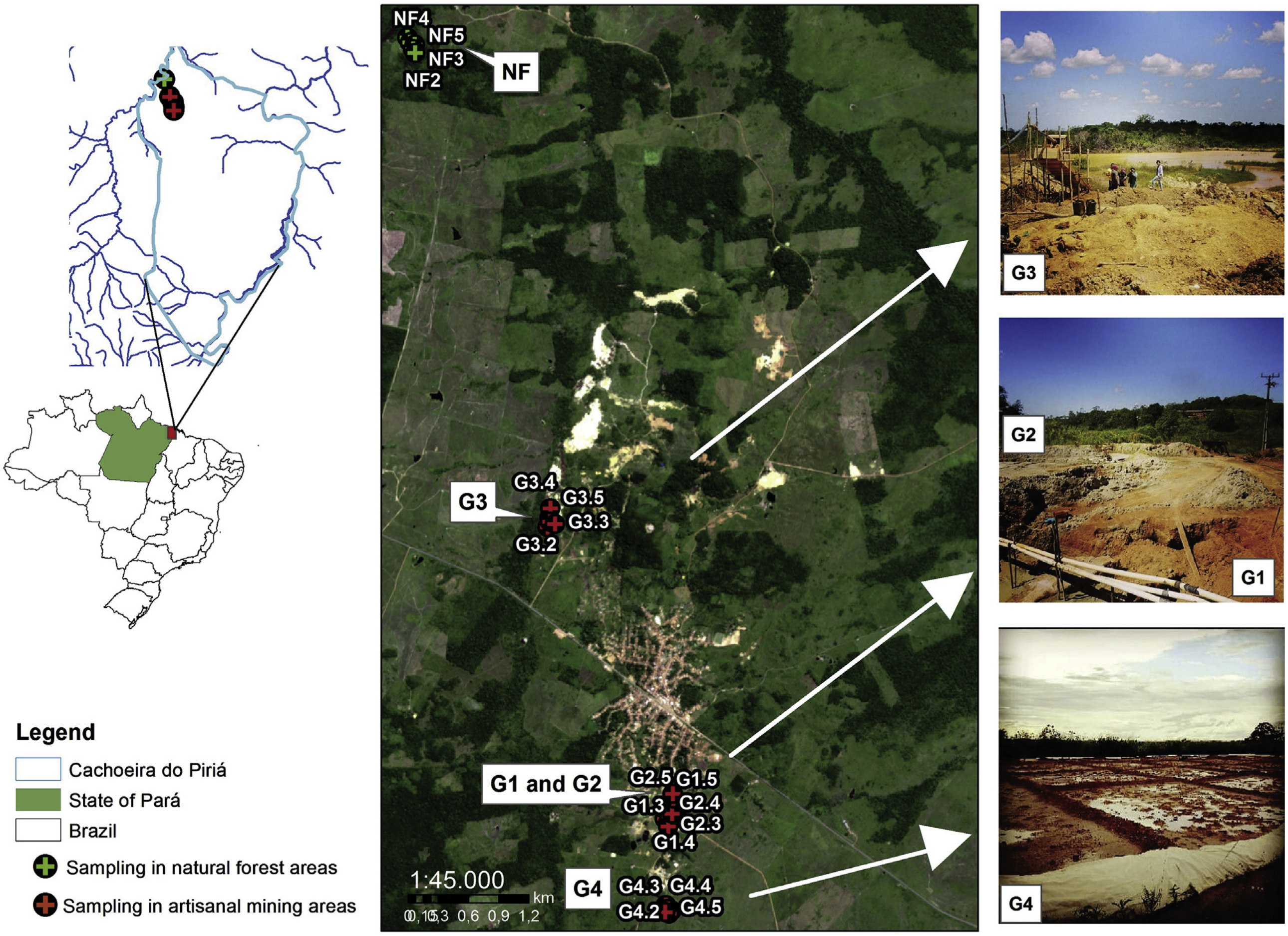

Fig. 2. Location map of sampling points in the studied areas.

the mixture of subsamples) represented a composite sample, that was air dried, sieved (Ø = 2 mm), and stored for chemical, physical, and mineralogical characterization.

2.3. Physical, chemical and mineralogical characterization

The sample pH was measured in a suspension at a soil-water ratio of 1:2.5. The exchangeable contents of calcium (Ca^{2+}), magnesium (Mg^{2+}), and aluminum (Al^{3+}) were extracted with KCl 1 mol L^{-1}. Ca^{2+} and Mg^{2+} were quantified by complexometry with 0.0125 mol L^{-1} EDTA and Al^{3+} by titration with 0.025 mol NaOH. Phosphorus (P) and potassium (K^{+}) were extracted with Mehlich 1 solution (0.05 HCl mol L^{-1} + H_2SO_4 0.0125 mol L^{-1}) and quantified by visible ultraviolet spectrophotometry and flame photometry, respectively. The organic carbon (OC) was quantified by digestion with potassium dichromate ($K_2Cr_2O_7$ 0.0667 mol L^{-1}) in sulfuric acid, and organic matter (OM) was estimated on the basis of total organic carbon (Teixeira et al., 2017a). Sorption complex results were used to calculate the cation exchange capacity (CEC), sum of bases (SB), base saturation (V%), and aluminum saturation (m%). The granulometry analysis was performed by the pipette method, with a solution of 0.1 mol NaOH as chemical dispersant under high speed mechanical agitation for 10 min. The clay fraction was separated by sedimentation, the sand by sieving, and the silt was calculated using the difference (Gee and Bauder, 1986).

The pseudototal concentrations of As were extracted by acid digestion in a microwave oven using royal water (HCl:HNO3 3:1) (McGrath and Cunliffe, 1985). A 0.5 g soil sample was weighed and placed in Teflon tubes, followed by addition of the acid solution. The digested extracts were diluted with ultrapure water to a final volume of 50 mL and filtered (PTFE 0.45 μm). Quantification was carried out by means of inductively coupled plasma mass spectrometry (ICP-MS, PerkinElmer) in triplicate. The same procedure was used to quantify the pseudototal content of iron (Fe) in the soil, in order to calculate pollution indices. The ERM® CC-141-certified reference material (FRM-free ground) and blank samples were used for quality assurance. The mean recovery for As was 82%, based on a certified value obtained with hydrofluoric acid extraction. These values are considered adequate for pseudototal extraction, as it is indicative of what can be released under normal environmental conditions of pH, temperature, and pressure (Rieuwerts et al., 2014).

The mineralogical characterization of the soil samples (0.15 mm fine fraction) was performed by PANalytical X'PERT PRO MPD (PW 3040/60) diffractometer powder method, with goniometer PW3050/60 (θ/θ), ceramic-ray tubes with copper anode ($K\alpha 1 = 1.540598$ Å), model PW3373/00, long fine focus (2200 W - 60 kV), Kβ nickel filter. The instrumental scanning conditions were: 4°–70°2θ, step size 0.02° 2θ and time/step of 10 s, divergent and automatic slit and anti-spreading of 4°; 10-mm mask; sample in circular motion with frequency of 1 rotation/s for all samples. Materials were identified using X-ray diffraction (XRD).

2.4. Pollution indices

In order to evaluate soil pollution, the enrichment factor (EF) and geoaccumulation index (Igeo) were calculated. The background value of the soil is usually used to calculate the pollution indexes (Kowalska et al., 2018). For this study, the natural forest was used as a reference area because of the higher contribution from mineral richness. Fe was used for geochemical normalization, since this metal has geochemical behavior similar to several PTEs and is considered a conservative element (Bhuiyan et al., 2010).

The EF of As was calculated using equation (1):

$$EF = (CAs / CFe)/(BAs / BFe) \tag{1}$$

where CAs is the concentration of As in the sample, CFe is the measured concentration of Fe in the same sample, BAs is the concentration of As in NF, and BFe is the concentration of Fe in NF. If $EF < 2$, there is depletion to minimum enrichment, $2 \leq EF < 5$ indicates moderate enrichment, $5 \leq EF < 20$ significant enrichment, $20 \leq EF < 40$ very high enrichment, and $EF > 40$ extremely high enrichment (Hakanson, 1980; Lin et al., 2019).

The geoaccumulation index (Igeo) is a geochemical parameter used to evaluate the pollution level in soils and sediments. In this study, Igeo was calculated by equation (2):

$$Igeo = \log_2(CAs / 1.5BAs) \tag{2}$$

where CAs is the measured concentration of As in the sample, BAs is the concentration of As in NF, and 1.5 is a constant. The Igeo values were interpreted according to Lin et al. (2019), where $Igeo < 0$ indicates unpolluted soil, $0 < Igeo < 1$ unpolluted to moderately polluted soil, $1 < Igeo < 2$ moderately polluted soil, $2 < Igeo < 3$ moderately to heavily polluted soil, $3 < Igeo < 4$ heavily polluted soil, $4 < Igeo < 5$ heavily to extremely polluted soil, and $Igeo > 5$ extremely polluted soil.

2.5. Chemical fractionation of As

The sequential extraction of As followed the methodology proposed by Drahota et al. (2014), which allows chemical fractionation of As into readily-soluble (F1), adsorbed (F2), amorphous mineral-linked arsenate (F3), crystalline mineral-linked arsenate (F4), and linked to sulfides/arsenides (F5) fractions. The F1 fraction was extracted with ultrapure water for 10 h (1:25 m/v); the F2 fraction was obtained with 0.01 mol ammonium monophosphate for 16 h (1:100 m/v); F3 fraction was extracted with 0.2 mol ammonium oxalate (in the dark, pH 3, stirred for 2 h); F4 fraction was obtained with 0.2 mol ammonium oxalate (pH 3 for 4 h at 80 °C); and F5 fraction was extracted with $KClO_3 + HCl + HNO_3$. Concentrations of As in the soil fractions were quantified by flame atomic absorption spectrometry (FAAS) (Thermo Scientific, model iCE 3000 series) with a hydride generator (Thermo Scientific, model VP100). For quality assurance, all extractions were performed in triplicate. The recovery of As was represented by the ratio between the sum of concentrations found in F1, F2, F3, F4, and F5 fractions and the total concentration of As, resulting in recovery rates of 86, 90, 89.31, 87.05, and 87.55% in G1, G2, G3, G4, and NF areas, respectively (Table 2S).

2.6. Oral bioaccessibility of As

The oral bioaccessibility of As was determined by the Simple Bioaccessibility Extraction Test (SBET), which simulates absorption in the gastric and intestinal phases of human ingestion (Mendoza et al., 2017). For gastric phase simulation, a sample was extracted with a glycine solution (0.4 mol L^{-1}) adjusted to pH 1.5, at a ratio of 1:100 (solid-liquid), and stirred for 1 h at 37 °C. A 10 mL aliquot was collected, centrifuged, filtered through a 0.45 mm membrane, and submitted for analysis of the dissolved As at this stage. The remaining solution was neutralized with Na_2CO_3 (pH 7), to simulate the passage from the gastric to intestinal phase, and the initial extractor volume was restored with 10 mL of 0.4 mol L^{-1} glycine (pH 7). At this stage, the solution was stirred for 3 h at 37 °C. A 10 mL aliquot was collected, centrifuged, and filtered by the same manner as in the gastric phase to determine dissolved As in the intestinal phase. Bioaccessible concentrations of As were quantified by FAAS (Thermo Scientific, model iCE 3000 series) with a hydride generator (Thermo Scientific, model VP100). For quality assurance, all extractions were performed in triplicate.

2.7. Assessment of environmental and human health risks

The potential ecological risk index (PERI), initially proposed for sediments by Hakanson (1980), is a method that comprehensively considers the potential impact of PTEs on ecosystems (Zhang et al., 2018). This method has been adopted in many studies to determine the ecological risk in soils and mining wastes (Kowalska et al., 2018; Lin et al., 2019; Tapia-Gatica et al., 2020; Xiao et al., 2019). In this study, PERI was calculated following equation (3):

$$PERI = T_{As} \left(\frac{C_{As}}{B_{As}}\right) \tag{3}$$

where TAs is the toxic-response factor for As (10) (Hakanson, 1980), CAs is the measured concentration of As in the sample, and BAs is the measured concentration of As in NF. Values of PERI were classified according to Hakanson (1980), for one element, where $PERI < 40$ indicates low ecological risk, $40 \leq PERI < 80$ moderate ecological risk, $80 \leq PERI < 160$ considerable ecological risk, $160 \leq PERI < 320$, high ecological risk, and $PERI > 320$ very high ecological risk.

The non-carcinogenic potential risk was based on the average daily dose (ADD) through three main pathways: ingestion (ADDing), inhalation (ADDinh), and dermal contact (ADDder), which allowed to estimate the hazard quotient (HQ) and hazard index (HI) for adults and children (USEPA, 2001). The HI was calculated according to Souza et al. (2017). For the carcinogenic potential risk, the ADD was multiplied by the corresponding sloping factor (SF) to produce a level of cancer risk (Lu et al., 2014) equations (4)–(10).

$$ADD\ ing = C\ x\ \frac{ingR\ x\ EF\ x\ ED}{BW\ x\ AT}\ x\ CF \tag{4}$$

$$ADD\ inh = C\ x\ \frac{inhR\ x\ EF\ x\ ED}{PEF\ x\ BW\ x\ AT} \tag{5}$$

$$ADD\ der = C\ x\ \frac{SL\ X\ SA\ X\ ABS\ x\ EF\ x\ ED}{BW\ x\ AT}\ x\ CF \tag{6}$$

$$HQ\ ing = ADD\ ing/Rfd\ (As) \tag{7}$$

$$HQ\ inh = ADD\ inh/Rfd\ (As) \tag{8}$$

$$HQ\ der = ADD\ der/Rfd\ (As) \tag{9}$$

$$HI = \sum HQ_i \tag{10}$$

where ADD (mg kg d^{-1}) = average daily dose; C (mg kg^{-1}) = As concentration; ingR (mg d^{-1}) = soil ingestion rate, 100 mg d^{-1} for adults and 200 mg d^{-1} for children (USEPA, 2001); InhR (m^3 day^{-1}) = inhalation rate, 7.6 m^3 day^{-1} for children and 20 m^3 day^{-1} for adults (Lu et al., 2014; USEPA, 2001); PEF (m^3 kg^{-1}) = particle emission factor, 1.36 × 10^9 m^3 kg^{-1} (USEPA, 2001); SL (cm^{-2} day^{-1}) = skin adherence factor, 0.2 mg cm^{-2} day^{-1} for children and for adults 0.875 cm^{-2} day^{-1} (USEPA, 2001); SA (cm^{-2}) = exposed skin area, 732 cm^2 for children and for adults 3202 cm^{-2} (USEPA, 2001); ABS = dermal absorption factor, 0.03 (Lu et al., 2014); EF (d y^{-1}) = exposure frequency, 279 days (Moreira et al., 2018); ED (y) = exposure duration, 24 h for adults and 4 h for children (Moreira et al., 2018); BW (kg) = body weight, 70 kg for adults and 16 kg for children (Moreira et al., 2018); AT = average time, with no carcinogenic effects (ED x 365 d); CF = conversion factor = 10^{-6} kg mg^{-1} (USEPA, 2001); Rfd = reference dose, 0.0003 for As (mg kg d^{-1}) (USEPA, 2001); and SF = sloping factor, 1.51 (Lu et al., 2014).

2.8. Statistical analysis and spatial distribution

Descriptive statistics were calculated for concentrations of As. The geochemical maps of As were created considering the World Geodetic System 1984 (WGS84). For the spatial interpolations of geochemical data, classical kriging algorithms and/or inverse distance weighting (PDI) extended by the application of some principles of fractal geometry (Multifractal IDW) were used (Lima et al., 2003). Interpolation was performed with ArcGis 10.2 software. Boxplot diagrams were used as reference for the choice of element distribution intervals (isoconcentrations curve). The relationship between bioaccessible As concentrations (gastric and intestinal phases), chemical fractions of As, and soil attributes, was evaluated through multiple regression equations obtained by the stepwise selection method, eliminating characteristics without statistical significance on bioaccessibility. All statistical analyzes were carried out using R (version 3.4.3) (R Core Team, 2017).

3. Results and discussion

3.1. Characterization of soils and mine tailings

The sample pH varied between mines and the native forest area (Table 1). In tailings from the G1 and G4 areas, the pH was alkaline to strongly alkaline (Souza et al., 2017). These rejects are derived from foliate, schist, metasedimentary, and metavolcanic rocks, whose quartz veins, as well as albite-quartz-sulfide changes and shear zones with quartz-carbonate-pyrite veins, where Au is found (Klein et al., 2017), consume H^+ ions during dissolution and generate aqueous carbonate species, increasing soil pH (Lindsay et al., 2015). Similar results were found in a mine of Au in Thailand (Chotpantarat et al., 2015) and in Serra Pelada, Pará (Teixeira et al., 2017b), with pH equal to 8.3 and 7.1, respectively. The authors attributed the alkaline pH to high base saturation and salt concentration, mainly calcium, magnesium, and sodium carbonates.

In the NF and G3 areas, the pH ranged from 4.2 to 5.8, characterizing high and medium acidity, respectively (Venegas et al., 1999). High soil acidity is common in tropical regions, where precipitation is intense and causes leaching of exchangeable bases from the superficial soil layers. In several soil classes under native forest from other regions of the state of Pará, pH was considered very acidic and ranged from 4.2 to 4.9 (Birani et al., 2015; Braz et al., 2013).

The OM content was low in the mining areas and medium in the forest area (Table 1) (Venegas et al., 1999). Low OM contents in tailings are related to losses during exploration of Au, as well as to the presence of PTEs at concentrations higher than those suitable for plant development (Fernandes et al., 2018), decreasing OM accumulation. Medium OM contents in the soil from the natural forest are a consequence of the climatic conditions, including high rainfall and temperature, which predominate in the Amazon region and contribute to the fast OM decomposition. The CEC was low in the tailings and medium in the NF area. The lower contents of exchangeable Al in the tailings may have contributed to low CEC in the mining areas. Higher CEC values were found in sediments from the southwestern Amazon, which was explained by high content of Al (Delarmelinda et al., 2017) and does not match that found in this study.

The sum of bases was lower in the mining areas than NF area, which is related to the lower OM content in the exploration areas and greater losses due to erosion and leaching. In the NF area, OM increases the concentration of exchangeable cations due to mineralization and contributes to retention of these elements in the soil by increasing CEC (Souza et al., 2015). In the G1 and G2 areas, the contents of K were below the detection limit. This element can be easily lost by leaching, that is favored by the high rainfall in the study region. The highest K content in NF is related to the highest CEC, which contributes to retention of this cation in the soil. In addition, the greater vegetation cover in this area reduces the losses of K by erosion (Chen et al., 2017).

The particle size distribution varied between the sampling areas (Table 1) due to the material used to extract Au. The high silt percentage in the G1 and G2 areas is associated to the intensive crushing of rocks, forming finer fractions to facilitate Au extraction. The sand fraction in G4 may be explained by the drainage and sedimentation of the silt fraction in the lagoons base, while sand remains on the top. The sand predominance in G3 is related to the formation of ore in conglomerate in colluvial and alluvial areas, with higher contents of sand than silt and clay. In NF, the sand content is according to the characteristics of the Amazon soils, predominantly sandy in the surface layer (Fernandes et al., 2018). This was also observed in forest and savanna areas in the state of Roraima, Amazon region (Matos et al., 2017).

3.2. Pseudototal concentrations of As

The levels of As varied between the mining areas, which is probably associated to the exploration types, mineralogy, technology, and beneficiation techniques (Fig. 3 and Table 2S). Extremely high concentrations of As, varying from 1560 to 10,000 mg kg^{-1}, were found in the tailings from G1, G2, and G4 areas (Fig. 3A, B, C, and Table 2S), which are from underground exploration at a depth of approximately 150 m. The excavation of deep layers, with different and higher contents of As, may have directly contributed to the high concentrations found in these tailings when compared to those from surface exploration (G3). Concentrations of As in tailings from mining areas in the United Kingdom also exceeded background and reference values, between 1 and 5 times, with concentration equal to 1.8 × 105 mg kg^{-1} in waste mines (Rieuwerts et al., 2014).

Among the rejects from the underground mines, concentrations of As were higher in the G2 area, followed by G1 (Fig. 3A and Table 2S). The lower content of As in the G1 area can be explained by the higher content of As associated with sulfide minerals, while in the G2 area, As is more associated with oxides (Fig. 4). Sulfides play a decisive role in the dynamics of As in soils and mine wastes. Under aerobic conditions, as found in the surface layer of sedimentation ponds, sulfides oxidize and release As, which may precipitate into secondary minerals in deeper layers or be leached (Kim et al., 2014). Inverse behavior occurs when As is associated with oxidic minerals, that are more resistant to weathering and

Table 1
Descriptive statistical analysis of physical and chemical attributes of tailings from underground mining with 13 years of disposal (G1), underground mining with 7 years of disposal (G2), colluvium mining (G3), cyanidation mining (G4), and soils from natural forest (NF).

Area		pH		OM	P	K	Ca	Mg	Al^{3+}	H + Al	SB	CEC[a]	V[b]	m[c]	Clay	Sand	Silt
		H_2O	KCl	$g\ kg^{-1}$	$mg\ dm^{-3}$	$cmol_c\ dm^{-3}$							%				
G1	Mean	7.45	7.02	10.26	0.77	<LD[f]	1.35	1.18	0.18	1.29	2.53	2.71	68.91	7.00	4.40	31.17	64.43
	Median	7.59	6.92	10.99	0.76	<LD	1.33	1.15	0.20	1.61	2.45	2.65	56.32	6.74	3.12	28.87	68.02
	Minimum	6.19	5.65	6.11	0.64	<LD	0.63	0.85	0.15	0.11	1.48	1.63	46.98	5.16	1.16	24.68	46.75
	Maximum	8.50	8.26	13.43	0.90	<LD	2.38	1.63	0.20	2.89	3.68	3.88	97.07	9.23	11.57	41.68	74.17
	SD[d]	0.90	1.09	2.82	0.11	<LD	0.60	0.27	0.02	1.04	0.75	0.77	21.82	1.35	3.80	6.11	9.86
	CV[e]	12.07	15.53	27.51	14.03	–	44.20	23.31	13.61	81.03	29.71	28.47	31.67	19.30	86.49	19.60	15.30
G2	Mean	8.73	8.60	12.95	2.03	<LD	0.77	0.70	0.14	0.44	1.47	1.61	75.76	8.81	0.42	26.75	72.83
	Median	8.74	8.64	12.21	2.17	<LD	0.70	0.83	0.15	0.50	1.53	1.73	73.33	7.89	0.50	24.74	74.76
	Minimum	8.53	8.43	10.38	0.14	<LD	0.43	0.48	0.10	0.22	0.95	1.05	65.56	7.22	0.10	19.02	63.56
	Maximum	8.82	8.70	17.71	3.65	<LD	1.10	0.83	0.20	0.56	1.93	2.08	88.75	11.59	0.60	36.34	80.63
	SD[d]	0.11	0.10	2.51	1.25	<LD	0.23	0.16	0.04	0.13	0.36	0.38	8.89	1.58	0.18	6.69	6.60
	CV[e]	1.22	1.11	19.43	61.75	–	29.71	23.02	26.73	28.50	24.54	23.96	11.74	17.98	42.99	25.00	9.06
G3	Mean	5.13	3.93	7.72	0.22	0.03	0.56	1.65	1.17	2.55	2.23	3.40	51.19	25.46	10.54	65.10	24.37
	Median	5.53	3.92	7.50	0.09	0.02	0.25	1.63	0.50	1.78	2.04	3.24	56.60	23.17	10.49	62.27	25.81
	Minimum	4.21	3.23	6.25	<LD	0.01	0.15	0.88	0.10	0.72	1.15	1.25	24.89	6.17	1.46	45.80	8.49
	Maximum	5.75	5.03	10.00	0.66	0.04	1.38	2.50	4.05	6.16	3.26	6.09	64.75	66.48	19.72	90.05	37.35
	SD[d]	0.62	0.62	1.31	0.25	0.01	0.46	0.54	1.47	1.88	0.81	1.68	14.27	21.76	7.87	19.51	11.83
	CV[e]	12.09	15.80	16.97	111.76	39.71	82.98	32.64	125.95	73.54	36.19	49.55	27.87	85.49	74.67	29.97	48.53
G4	Mean	8.60	8.50	8.62	1.91	0.03	1.05	0.84	0.12	0.38	1.92	2.04	83.60	5.88	0.95	89.97	9.09
	Median	8.60	8.50	8.75	1.92	0.03	1.00	0.88	0.10	0.33	1.90	2.10	85.06	5.01	1.01	89.88	8.98
	Minimum	8.51	8.37	8.12	1.25	0.02	1.00	0.63	0.10	0.28	1.66	1.76	78.86	4.52	0.50	89.04	8.04
	Maximum	8.75	8.63	8.75	2.82	0.05	1.25	1.08	0.20	0.50	2.11	2.21	88.07	9.51	1.21	91.45	10.15
	SD[d]	0.09	0.09	0.25	0.52	0.01	0.10	0.15	0.04	0.08	0.16	0.16	3.29	1.86	0.27	0.82	0.68
	CV[e]	1.02	1.05	2.90	27.38	29.19	9.52	17.82	33.33	21.61	8.19	7.83	3.94	31.67	28.23	0.91	7.51
NF	Mean	4.86	4.11	39.36	0.32	0.14	1.31	1.49	1.30	7.79	2.94	4.24	30.28	28.79	6.78	63.52	29.70
	Median	4.91	4.21	40.61	0.29	0.15	1.00	1.50	0.55	5.99	2.97	3.95	29.13	13.93	6.34	62.53	28.16
	Minimum	4.47	3.52	25.62	0.19	0.08	0.38	1.00	0.40	4.27	1.96	3.42	12.62	8.71	5.43	53.89	22.71
	Maximum	5.38	4.71	52.49	0.59	0.19	2.38	2.13	3.30	15.10	4.19	5.48	44.03	60.21	9.30	71.86	39.32
	SD[d]	0.35	0.40	9.48	0.15	0.04	0.77	0.39	1.13	3.88	0.82	0.73	11.40	21.08	1.34	6.72	6.44
	CV[e]	7.12	9.81	24.07	45.57	32.00	58.79	25.92	86.65	49.79	27.73	17.19	37.64	73.23	19.72	10.57	21.69

[a] Effective cation exchange capacity.
[b] Base saturation.
[c] Aluminium saturation.
[d] Standard deviation.
[e] Coefficient of variation.
[f] Below the detection limit.

suffer less losses to the environment, as found in the G2 area.

In the waste deposits, there are no waterproofing agents and proper management. These wastes contain residual minerals (including sulfur minerals) that are exposed to the weather conditions and rainwater drainage. The high rainfall of the region favors losses of chemical elements from the tailings through leaching and erosion. In addition, these tailings are predominantly formed by sand-sized particles, which facilitates oxygen diffusion throughout the profile, as well as mineral oxidation, especially in the sulfides found in G1, leading to solubilization and possible leaching of As. The heterogeneity in the contents of As in tailings submitted to similar exploration processes may be explained by mineralogical variations and differentiated exposure periods. The underground mine reaches a depth of approximately 150 m, implying in different mineralogical compositions with varied mineral sources of As (Fig. 4S). Depending on the type of host rocks and the intensity of hydrothermal changes, such variations are common in deposits of Au (Melo et al., 2014). Losses of As can bring risks to the environment and human health due to contamination of water, soil, and plants. The concentrations of As in the artisanal mining tailings from Cachoeira do Piriá are higher than those reported by Souza et al. (2017) in Serra Pelada, Brazil, and by Ding et al. (2016) in China.

The concentrations of As in the G4 area were lower than the average values found in G1 and G2. The G4 tailings, which are from reprocessing of underground mining tailings, showed a mean concentration of As equal to 1844 mg kg^{-1} (Fig. 3C and Table 2S), which is approximately 1.5 and 3 times lower than the concentration found in the G1 and G2 areas, respectively. These results may be related to the lower occurrence of As-rich minerals, as well as the higher occurrence of low stability sulfide minerals in the G4 area (Fig. 4S).

Lower levels of As in the G4 area than in G1 and G2 may also be attributed to losses by erosion and leaching. Reprocessing of underground mine tailings depends on the demand of the prospectors and may take years to occur. The exposure time to environmental conditions in which the underground tailings are submitted before being reprocessed can lead to losses of As, reducing the concentrations in these wastes, which also explains the higher levels observed in the G2 area than in G1. Another process that can lead to loss of As is volatilization, which can occur in tailings ponds before the cyanide process, and during the processing of Au with cyanide. During the ore roasting, As from the sulfide minerals is oxidized to As_2O_3 and can be lost to atmosphere, which reduces the contents of this metalloid in the tailings. Leaching of soluble oxyanions, generated during roasting, can also lead to losses of As. The occurrence of As-rich minerals, as well as precipitation of As during cyanidation (Kyle et al., 2012), may contribute to maintenance of As in G4.

In the NF area, the mean concentrations of As varied between 0.7 and 6 mg kg^{-1} (Fig. 3D). These results are similar to those found for the state of Pará in native forest areas, without anthropic interference (Fernandes et al., 2018). In Au mining areas, the concentrations of As are usually higher than those found in areas with

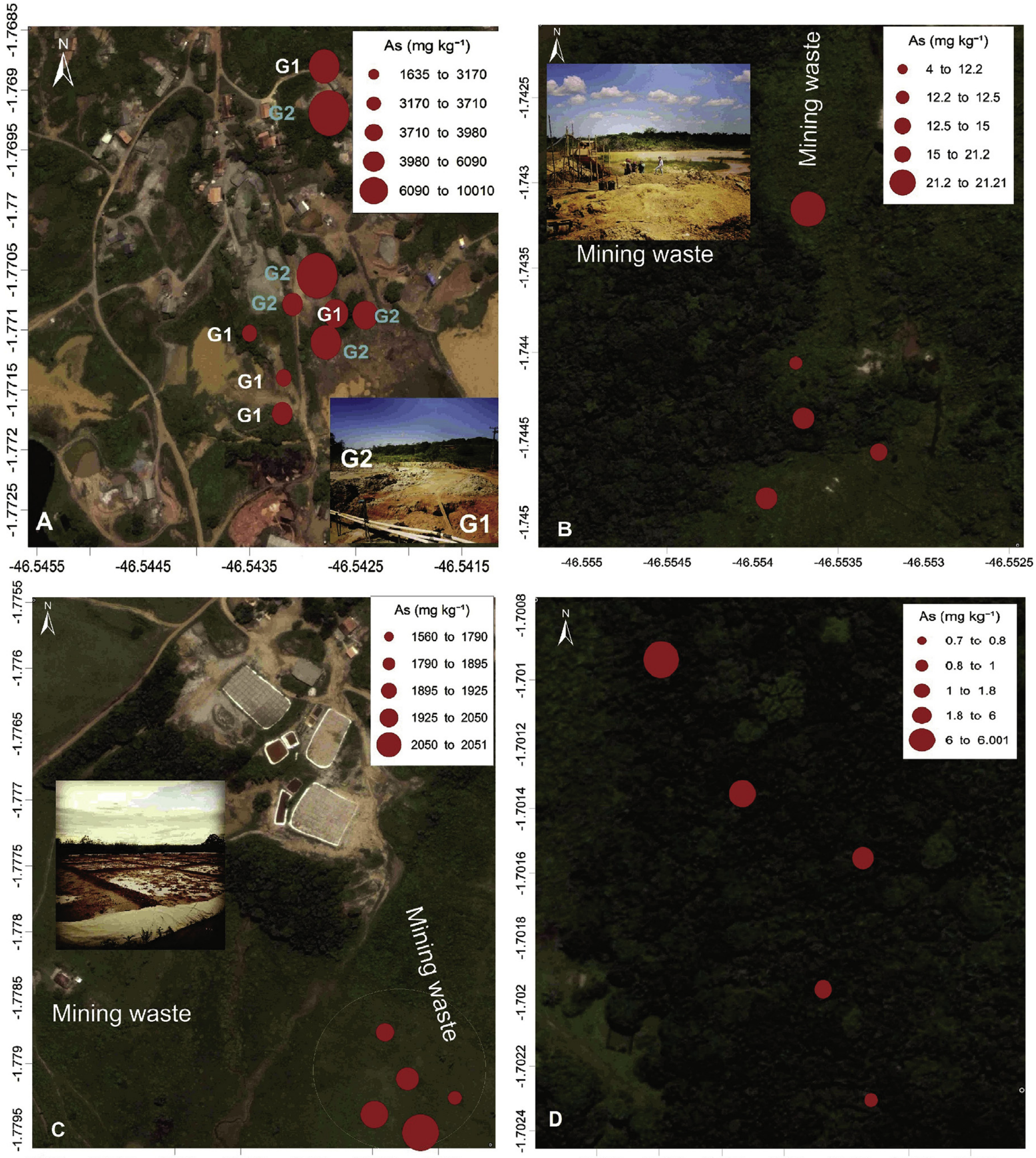

Fig. 3. Spatial distribution of As concentrations in tailings from underground mining with 13 years of disposal (G1) - A, underground mining with 7 years of disposal (G2) - A, colluvium mining (G3) - B, cyanidation mining (G4) - C, and soils from natural forest (NF) - D.

lower mineral potential. Occurrence of As sulfide minerals in Au mining areas was observed in Brazil by Souza et al. (2017) in Serra Pelada, Amazon region, in Colombia by Desbarats et al. (2015), and in China by Ding et al. (2016).

3.3. *Pollution assessment*

The pollution indices indicate that all mining areas had significant processes of enrichment and accumulation of As (Table 2). The EF showed that there is extremely high enrichment in the underground tailings (G1, G2, and G4) and low enrichment in the tailings from the G3 area according to Lin et al. (2019). The Igeo indicated geoaccumulation of As in all mining areas and, on the basis of this indicator, the G3 tailings are moderately to heavily polluted, and G1, G2, and G4 tailings are extremely polluted (Lin et al., 2019).

Areas of Au exploration in the Amazon are recognized for generating large amounts of tailings with high PTEs levels (Teixeira et al., 2018), which generally leads to enrichment and environmental contamination by these elements. The results found in this study suggest the need of environmental control mechanisms in order to avoid environmental and human health risks by As contamination. In other areas of Au exploitation in the Amazon (Serra Pelada), the EF indicated enrichment by anthropic sources (Teixeira et al., 2018) and Igeo suggested that the area was

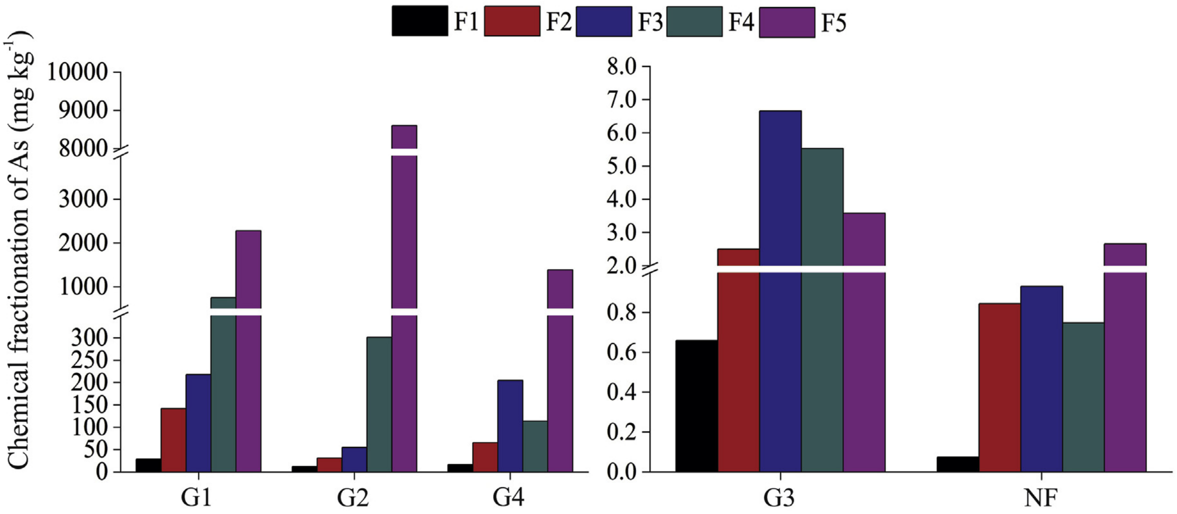

Fig. 4. Chemical fractionation of As into readily-soluble (F1), adsorbed (F2), amorphous mineral-linked arsenate (F3), crystalline mineral-linked arsenate (F4), and linked to sulfides/arsenides (F5) fractions of tailings from underground mining with 13 years of disposal (G1), underground mining with 7 years of disposal (G2), colluvium mining (G3), cyanidation mining (G4), and soils from natural forest (NF).

Table 2
Enrichment factor (EF), geoaccumulation index (Igeo), and potential ecological risk index (PERI) of As concentrations in tailings from underground mining with 13 years of disposal (G1), underground mining with 7 years of disposal (G2), colluvium mining (G3), cyanidation mining (G4), and soils from natural forest (NF).

Area	Pollution indexes		
	EF	Igeo	PERI
G1	163.3	9.9	14131.0
G2	644.1	10.8	26524.0
G3	5.3	2.1	64.0
G4	130.5	9.2	8951.0
NF	1.0	−0.6	10.0

moderately contaminated (Souza et al., 2017).

3.4. Chemical fractionation of As

Chemical fractionation of PTEs is essential because it indicates the origin, mobility, and bioavailability of these elements (Fernández-Ondoño et al., 2017; Pérez-Moreno et al., 2018; Sah et al., 2019), as well as the current and potential contamination of soils, tailings and sediments. In the studied areas, tailings showed low percentages of As in the highest mobility fraction (F1), varying between 0.12 and 3.11% of the pseudototal As (Table 3S). However, these low percentages represent amounts of As equal to 28.77 (G1), 16.47 (G4), and 11.9 mg kg^{-1} (G2) (Fig. 4), which are 20, 11, and 8-fold higher, respectively, than the QRV of As for soils in the state of Pará (Fernandes et al., 2018), which is based on the total concentration. In G3, 3.11% of the pseudototal As was found in the F1 fraction, corresponding to only 0.66 mg kg^{-1}, that is readily available for plant absorption and, therefore, may not be neglected. The F1 fraction is considered the most toxic to the environment and may carry environmental risk to surrounding areas through dispersion of soil, tailings and water (Drahota et al., 2014; Mensah et al., 2020). The low values of As in the F1 fraction (in relation to pseudototal content of As) may be explained by losses through leaching as a consequence of the frequent and intense rainfall in the Amazon region (Moreira et al., 2018; Pereira et al., 2020).

In the F2 fraction (adsorbed As), percentages equal to 11.8 (G3), 3.57 (G1), 3.19 (G4), and 0.31% (G2) (Table 3S) of the pseudototal content were found, representing 2.5, 141.93, 65.5, and 31.44 mg kg^{-1} (Fig. 4), respectively. These values are very high and potentially bioavailable (Pérez-Moreno et al., 2018; Sah et al., 2019), indicating that As may cause serious damage to environment and population health. When considering F1 + F2 fractions, which are usually adopted to assess the bioavailability and mobility of PTEs (Sun et al., 2014; Sah et al., 2019), an extremely worrying scenario is observed in the mining areas, mainly because in tropical regions these fractions may be easily mobilized (Moreira et al., 2018).

Relatively significant percentages of As were found in the F3 and F4 fractions of tailings (Fig. 4 and Table 3S). In G1 and G2 tailings, there is predominance of As in the F4 fraction (18.88%) when compared to F3 (5.47%), indicating greater binding of As with amorphous Fe oxides. In G3 and G4, there is higher association of As with the F3 fraction than with F4, suggesting the predominance of As bound to crystalline Fe oxides and arsenates in relation to amorphous Fe oxides. These results indicate that the dynamics of As in tailings, in the F3 and F4 fractions, is highly influenced by the specific surface and crystallinity of Fe oxides (Bissen and Frimmel, 2003; Drahota et al., 2014; Mensah et al., 2020).

The F5 fraction predominated in G1, G2, and G4, with 57.36, 86, and 67.52% of pseudototal As (Fig. 4 and Table 3S), respectively, suggesting that much of As is strongly linked to crystalline structures of minerals which contain As (Fig. 4S). On the other hand, in the G3 tailings, the association with the F3 fraction was higher, indicating greater activity of low-crystallinity Fe oxides. The results found in G3 may be explained by the greater wear of the source material in the exploration process, involving frequent use of water and intense soil revolving (Fig. 2S), as well as more acidic pH, which contributes to dilution and transfer of As to other fractions (Ali et al., 2017). In the NF area, As showed the lowest association with all fractions, indicating lower potential risk under natural conditions due to low anthropogenic influence.

Higher association of As with all non-residual fractions was found in G1 than in G2. The greater exposure time of G1, considering the intense weathering in the Amazon region (Souza et al., 2017), may explain the high mobilization of As, including for F1 and F2 (28.77 and 141.93 mg kg^{-1}, respectively), indicating that the risks to environment and human health may increase according to the exposure time of tailings. High content of As in the most mobile fraction was also observed by Mensah et al. (2020), studying soil from an abandoned mine, where similar results were found. In soils from Germany (Shaheen et al., 2017) and Italy (Giacomino et al., 2010), as well as in Au mining areas in Minas Gerais, Brazil (Ono et al., 2015), high As values were also observed in mobile fractions.

3.5. Oral bioaccessibility of As

Bioaccessible concentrations of As were found in all areas studied, both in the intestinal and gastric phases (Fig. 5). Although in low percentages of the total concentrations, the bioaccessibility of As is high in the G1, G2, and G4 areas, which may be associated with the high concentrations in bioavailable fractions (Fig. 4). Higher bioaccessibility of As indicates greater potential risk for human health through ingestion of contaminated soil or sediment (Fernández-Caliani et al., 2019). High total concentrations of As and low bioaccessible percentage in mine soils have been reported by Fernández-Caliani et al. (2019) in Spain, Li et al. (2015) in China, and Ono et al. (2012) in an Au mine in Brazil.

For G3 and NF areas, which had the lowest total content of As, higher percentage bioaccessibility was found in the gastric phase, while in the G1, G2, and G4 areas, higher bioaccessibility occurred in the intestinal phase. High dissolved As amounts in the gut indicate a potential health risk, given that metal absorption occurs mainly in this organ (Ono et al., 2012). Higher bioaccessibility in the gastric phase was reported by Juhasz et al. (2014), due to the induced desorption of As linked to oxides at extremely acidic pH (±1.5). High acidity contributes to solubilization of Fe oxides and As source minerals with high Fe concentrations (Juhasz et al., 2011; Li et al., 2015). Soluble Fe migrating to the intestine, which has a basic pH, may precipitate as amorphous Fe and adsorb part of the solubilized As in the gastric phase, reducing bioaccessibility.

In accordance with the results obtained in the G1, G2, and G4 areas, greater bioaccessibility of As in the intestinal phase was observed by Wragg et al. (2011). Such results can be attributed to dissolution of Fe by action of organic acids, such as citrate, present in the intestinal fluid, which decreases the formation of amorphous Fe, reducing the adsorption of As (Juhasz et al., 2014), or due to chemical precipitation with cations in the intestine (Fernández-Caliani et al., 2019). Another mechanism that explains the higher level of As dissolved in the intestinal phase is the chemical speciation of this element. If As^{5+} is the predominant species in the soil, it is more likely to be absorbed in the gut compared to the stomach. As^{5+} is phosphate analogous (HPO_4^{2-}) and, therefore, can be absorbed by the same metabolic pathway. Phosphate is highly absorbed by the intestinal system, mainly by the duodenum and to a lesser extent by the jejunum and ileum (Beak et al., 2006). These results suggest that gastrointestinal bioaccessibility varies according to the chemical soil properties, due to the dominance of sorbed surfaces (Kim et al., 2002).

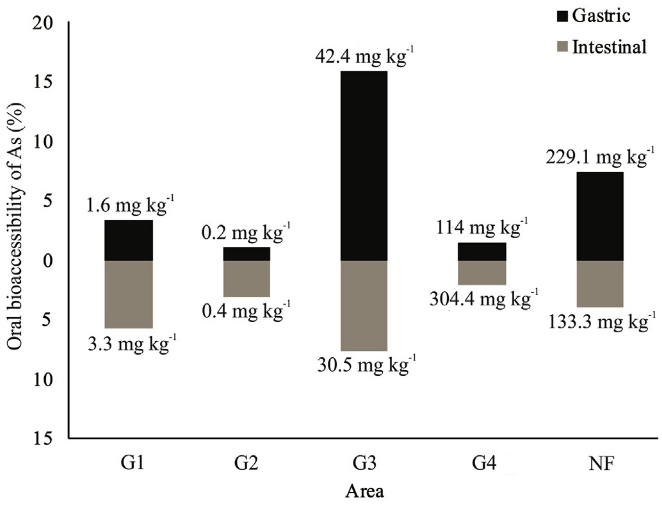

Fig. 5. Oral bioaccessibility of As in tailings from underground mining with 13 years of disposal (G1), underground mining with 7 years of disposal (G2), colluvium mining (G3), cyanidation mining (G4), and soils from natural forest (NF).

The bioaccessible concentration of As in the gastric phase showed a positive correlation ($r^2 = 0.99$) with As in soluble, adsorbed and linked to arsenide/sulfide fractions (Table 3), indicating that these fractions may be solubilized at pH 1.5 (Li et al., 2014). OM and amorphous fraction were negatively correlated, which can be explained by their greater binding strength with As, reducing the solubility at pH 1.5 (Mendoza et al., 2017) and promoting the formation of stable and not soluble complexes.

In the intestinal phase, the bioaccessible As was negatively correlated with the soluble and adsorbed fractions of this metalloid, which may be due to solubilization of As in the gastric phase, resulting from the formation of complexes at basic pH (Li et al., 2014). On the other hand, the positive correlations of bioaccessible As with the amorphous and crystalline fractions, pH and OM, can be attributed to solubilization and complexation of As in the intestinal phase, with formation of HCO_{3-}, that reduces the As precipitation with oxides at high pH (Mendoza et al., 2017).

3.6. Risks to environment and human health

PERI allows measuring the sensitivity of the biological community to general contamination caused by PTEs in a given location (Hakanson, 1980). This index is robust and, therefore, may be used to indicate the ecological risk in Au exploration areas in the Amazon, since PERI has been used to assess potential risks to environmental quality in agricultural and natural soils, sediments, and mine tailings (Duodu et al., 2016; Jiang et al., 2019; Ngole-Jeme and Fantke, 2017; Tapia-Gatica et al., 2020; Xiao et al., 2019; Pereira et al., 2020). In the mining areas, values of PERI varied between 10 and 26,524, following the order G2 > G1 > G4 > G3 > NF. In G2, G1, and G4, the values of PERI were approximately 88, 44, and 28 times higher, respectively, than the value which indicates very high ecological risk according to Hakanson (1980). The ecological risk is moderate in G3 and low in NF. Despite the moderate risk in G3, the pseudototal concentrations of As (21.2 mg kg^{-1}) (Table 2S) deserve attention, since they are 16 times higher than the background value for soils in the state of Pará (Fernandes et al., 2018). In Pakistan, exposure to 13.9 mg kg^{-1} of As (concentration lower than the found in G3) altered the bacterial community composition and affected individuals resistant to this metalloid (Sheik et al., 2012). In Krugersdorp soils, South Africa, high ecological risk was observed as a consequence of Au exploration (Ngole-Jeme and Fantke, 2017). The results found in this study indicate high risk to biodiversity, as well as increased difficult for revegetation of the areas, which contributes with leaching and erosion to distant areas and rivers.

Values of HI higher than 1 represent high non-carcinogenic risk to human health (Hu et al., 2012; Souza et al., 2017). The NF and G3 areas showed low non-carcinogenic risk for both children and adults, which can be explained by the lower pseudototal concentrations of As observed in these areas (Table 2S). On the other hand, in the G2, G1, and G4 areas, the non-carcinogenic risk index (HI) for children and adults ranged from 1.2 to 17.8 (Fig. 6A), indicating potential risk to the health of adults and children (Liu et al., 2013) in function of As contamination. This element may enter in the human body through ingestion, inhalation, and direct contact with contaminated soil (Hu et al., 2012; Park and Choi, 2013), maily in

Table 3
Multiple regression equations for estimation of oral bioaccessibility of As in gastric and intestinal phases.

Phase	Equation	R^2	*p*
Gastric	$B_{As} = ASo*1.795685 + AAd*1.015522 - AAm*0.395856 + AArSu*0.009406 - OM*0.059641 + 2.851498$	0.99	<0.01
Intestinal	$B_{As} = -ASo*17.739 - AAd*3.581 + AAm*1.031 + ACr*1.063 + pH*70.832 + OM*1.534-394.920$	0.99	<0.01

B_{As}, arsenic bioaccessibility; ASo, readily-soluble arsenic; AAd, arsenic adsorbed; AAm, arsenic linked to amorphous oxides; AArSu, arsenic bound to arsenides/sulfides; OM, organic matter; ACr, arsenic bound to crystalline oxides.

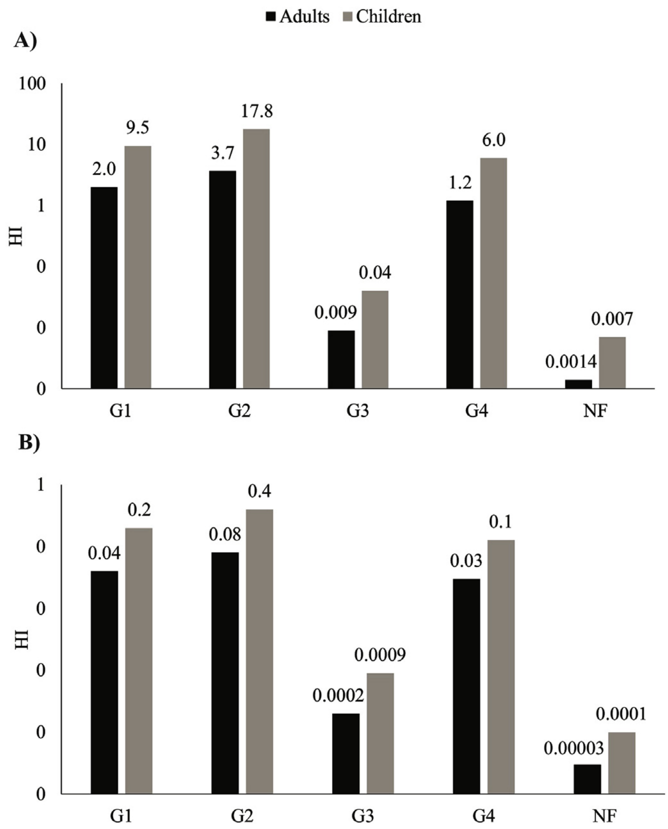

Fig. 6. Non-carcinogenic (A) and carcinogenic (B) hazard indices for adults and children in underground mining tailings with 13 years of disposal (G1), underground mining tailings with 7 years of disposal (G2), colluvium mining (G3), cyanidation mining (G4), and soils from natural forest (NF).

cases of accidental ingestion of soil by children, due to frequent hand-to-mouth movement and lower body weight (Izquierdo et al., 2015; Souza et al., 2017).

For carcinogenic HI, 10^{-4} is the value taken as the parameter to establish if there is carcinogenic risk (Liu et al., 2013). NF and G3 areas had carcinogenic HI lower than the acceptable limit for children and adults (except G3 that presented HI > 10^{-4} for children), suggesting that there is no carcinogenic risk to adults in these areas (Fig. 6B). On the contrary, G2, G1, and G4 areas showed HI extremely higher than the acceptable value for both children and adults, varying from 0.03 to 0.4, indicating high health risk, especially for children. In all areas, carcinogenic HI was higher for children, which is due to greater direct contact with soil particles (Park and Choi, 2013). These results allow to state that both adults and children deserve attention. However, children deserve special attention because they are more susceptible to carcinogenic and non-carcinogenic risks in the study area.

Potential health risks in the areas of waste deposit in Cachoeira do Piriá (Fig. 6A and B) are higher than previously described risks in Serra Pelada, Brazil (Souza et al., 2017), and Nanjing and Xikuangshan, China (Li et al., 2014). Sources of As, including mining waste and source material, when combined, may expose communities to an endemic contamination risk by As (Ramirez-andreotta et al., 2013). The high HI values in the studied Au mining areas indicate that human exposure to high concentrations of As can cause damage to the health of the local population and environment.

4. Conclusions

The wastes from Au mining areas studied in the eastern Amazon are highly contaminated with As, mainly through the prolonged exposure time. The concentrations found are well above the background and quality reference values used to assess environmental and human health risks according to environmental agencies. Mine tailings are highly polluted because of high enrichment, accumulation, and contamination by As, indicating high environmental risk. Serious health risks for children and adults were evidenced from the non-carcinogenic risk indices, which reached up to 17.8, well above the acceptable limit (1.0), in addition to a high carcinogenic risk for both children and adults. The oral bioaccessibility found in gastric and intestinal phases is extremely worrying and was corroborated by the high reactive fractions in three mining areas, suggesting that high concentrations of As may be absorbed by local population. The results show that the study area is polluted because of Au mining, putting the environment and health of the population at risk, and that there is an urgent need for intervention by environmental control agencies to remediate the waste.

Declaration of competing interest

The authors declare that they have no known competing financial interests or personal relationships that could have appeared to influence the work reported in this paper.

CRediT authorship contribution statement

Hamilton Ferreira de Souza Neto: Methodology, Investigation, Writing - original draft. **Wendel Valter da Silveira Pereira:** Conceptualization, Methodology, Writing - review & editing. **Yan Nunes Dias:** Methodology, Writing - original draft. **Edna Santos de Souza:** Writing - review & editing, Data curation. **Renato Alves Teixeira:** Writing - review & editing, Investigation. **Mauricio Wilians de Lima:** Formal analysis, Methodology. **Silvio Junio Ramos:** Resources, Writing - review & editing. **Cristine Bastos do Amarante:** Resources, Data curation. **Antonio Rodrigues Fernandes:** Resources, Funding acquisition, Writing - review & editing, Data curation.

Acknowledgements

We thank the Brazil's National Counsel of Technological and Scientific Development (CNPq) for financial support (425312/2018-6 and 305819/2018-6), and Coordination for the Improvement of Higher Education Personnel (CAPES) for the financial support in the development of this work and for the scholarships provided.

Appendix A. Supplementary data

Supplementary data to this article can be found online at https://doi.org/10.1016/j.envpol.2020.114969.

References

Ali, J., Kazi, T.G., Afridi, H.I., Baig, J.A., Shah, F., Arain, M.S., 2017. Evaluates the chemical fractions of arsenic bounded to solid matrixes of thar coalfield of Pakistan by sequential extraction method. Environ. Prog. Sustain. Energy 36, 1667–1675. https://doi.org/10.1002/ep.12624.

Beak, D.G., Basta, N.T., Scheckel, K.G., Traina, S.J., 2006. Bioaccessibility of arsenic (V) bound to ferrihydrite using a simulated gastrointestinal system. Environ. Sci. Technol. 40, 1364–1370. https://doi.org/10.1021/es0516413.

Bhuiyan, M.A.H., Parvez, L., Islam, M.A., Dampare, S.B., Suzuki, S., 2010. Heavy metal pollution of coal mine-affected agricultural soils in the northern part of Bangladesh. J. Hazard Mater. 173, 384–392. https://doi.org/10.1016/j.jhazmat.2009.08.085.

Birani, S.M., Fernandes, A.R., Braz, A.M. de S., Pedroso, A.J.S., Alleoni, L.R.F., 2015. Available contents of potentially toxic elements in soils from the Eastern Amazon. Geochemistry 75, 143–151. https://doi.org/10.1016/j.chemer.2015.01.001.

Bissen, M., Frimmel, F.H., 2003. Arsenic — a review. Part I: occurrence, toxicity, speciation, mobility. Acta Hydrochim. Hydrobiol. 31, 9–18. https://doi.org/10.1002/aheh.200390025.

Braz, A.M. de S., Fernandes, A.R., Ferreira, J.R., Alleoni, L.R.F., 2013. Distribution coefficients of potentially toxic elements in soils from the eastern Amazon. Environ. Sci. Pollut. Res. 20, 7231–7242. https://doi.org/10.1007/s11356-013-1723-9.

Bundschuh, J., Maity, J.P., Nath, B., Baba, A., Gunduz, O., Kulp, T.R., Jean, J.-S., Kar, S., Yang, H.-J., Tseng, Y.-J., Bhattacharya, P., Chen, C.-Y., 2013. Naturally occurring arsenic in terrestrial geothermal systems of western Anatolia, Turkey: potential role in contamination of freshwater resources. J. Hazard Mater. 262, 951–959. https://doi.org/10.1016/j.jhazmat.2013.01.039.

Castilhos, Z., Rodrigues-Filho, S., Cesar, R., Rodrigues, A.P., Villas-Bôas, R., Jesus, I., Lima, M., Faial, K., Miranda, A., Brabo, E., Beinhoff, C., Santos, E., 2015. Human exposure and risk assessment associated with mercury contamination in artisanal gold mining areas in the Brazilian Amazon. Environ. Sci. Pollut. Res. 22, 11255–11264. https://doi.org/10.1007/s11356-015-4340-y.

Chatterjee, D., Adak, S., Banerjee, N., Bhattacharjee, P., Bandyopadhyay, A.K., Giri, A.K., 2018. Evaluatıon of health effects, genetıc damage and telomere length ın children exposed to arsenic in West Bengal, India. Mutat. Res. Genet. Toxicol. Environ. Mutagen 836, 82–88. https://doi.org/10.1016/j.mrgentox.2018.06.012.

Chen, J., Wei, F., Zheng, C., Wu, Y., Adriano, D.C., 1991. Background concentrations of elements in soils of China. Water Air Soil Pollut. 57–58, 699–712.

Chen, S., Yan, Z., Chen, Q., 2017. Estimating the potential to reduce potassium surplus in intensive vegetable fields of China. Nutrient Cycl. Agroecosyst. 107, 265–277. https://doi.org/10.1007/s10705-017-9835-0.

Chotpantarat, S., Chunhacherdchai, L., Wikiniyadhanee, R., Tongcumpou, C., 2015. Effects of humic acid amendment on the mobility of heavy metals (Co, Cu, Cr, Mn, Ni, Pb, and Zn) in gold mine tailings in Thailand. Arab. J. Geosci. 8, 7589–7600. https://doi.org/10.1007/s12517-014-1750-y.

Cordeiro, I.M.C.C., Rangel-Vasconcelos, L.G.T., Schwartz, G., Oliveira, F.A. (Eds.), 2017. Nordeste Paraense: panorama geral e uso sustentável das florestas secundárias. Embrapa Amazônia Oriental, Belém.

Coufalík, P., Mikuska, P., Matousek, T., Vecera, Z., 2016. Determination of the bioaccessible fraction of metals in urban aerosol using simulated lung fluid. Atmos. Environ. J. 140, 469–475. https://doi.org/10.1016/j.atmosenv.2016.06.031.

Delarmelinda, E.A., Souza Júnior, V.S., Wadt, P.G.S., Deng, Y., Campos, M.C.C., Câmara, E.R.G., 2017. Soil-landscape relationship in a chronosequence of the middle Madeira River in southwestern Amazon, Brazil. Catena 149, 199–208. https://doi.org/10.1016/j.catena.2016.09.021.

Desbarats, A.J., Parsons, M.B., Percival, J.B., 2015. Arsenic mobility in mildly alkaline drainage from an orogenic lode gold deposit, Bralorne mine, British Columbia. Appl. Geochem. 57, 45–54. https://doi.org/10.1016/j.apgeochem.2014.11.015.

Ding, H., Ji, H., Tang, L., Zhang, A., Guo, X., Li, C., Gao, Y., Briki, M., 2016. Heavy metals in the gold mine soil of the upstream area of a metropolitan drinking water source. Environ. Sci. Pollut. Res. 23, 2831–2847. https://doi.org/10.1007/s11356-015-5479-2.

Drahota, P., Grösslová, Z., Kindlová, H., 2014. Selectivity assessment of an arsenic sequential extraction procedure for evaluating mobility in mine wastes. Anal. Chim. Acta 839, 34–43. https://doi.org/10.1016/j.aca.2014.06.022.

Duodu, G.O., Goonetilleke, A., Ayoko, G.A., 2016. Comparison of pollution indices for the assessment of heavy metal in Brisbane River sediment. Environ. Pollut. 219, 1077–1091. https://doi.org/10.1016/j.envpol.2016.09.008.

Faial, K., Deus, R., Deus, S., Neves, R., Jesus, I., Santos, E., Nahum, C., Brasil, D., 2015. Mercury levels assessment in hair of riverside inhabitants of the Tapajós River, Pará State, Amazon, Brazil: fish consumption as a possible route of exposure. J. Trace Elem. Med. Biol. 30, 66–76. https://doi.org/10.1016/j.jtemb.2014.10.009.

Fernandes, A.R., Souza, E.S. de, de Souza Braz, A.M., Birani, S.M., Alleoni, L.R.F., 2018. Quality reference values and background concentrations of potentially toxic elements in soils from the Eastern Amazon, Brazil. J. Geochem. Explor. 190, 453–463. https://doi.org/10.1016/j.gexplo.2018.04.012.

Fernández-Caliani, J.C., Giráldez, M.I., Barba-Brioso, C., 2019. Oral bioaccessibility and human health risk assessment of trace elements in agricultural soils impacted by acid mine drainage. Chemosphere 237, 124441. https://doi.org/10.1016/j.chemosphere.2019.124441.

Fernández-Ondoño, E., Bacchetta, G., Lallena, A.M., Navarro, F.B., Ortiz, I., Jiménez, M.N., 2017. Use of BCR sequential extraction procedures for soils and plant metal transfer predictions in contaminated mine tailings in Sardinia. J. Geochem. Explor. 172, 133–141. https://doi.org/10.1016/j.gexplo.2016.09.013.

Gee, G.W., Bauder, J.W., 1986. Particle-size analysis. In: Klute, A. (Ed.), Methods of Soil Analysis. American Society of Agronomy, Madison, pp. 383–411.

Giacomino, A., Malandrino, M., Abollino, O., Velayutham, M., Chinnathangavel, T., Mentasti, E., 2010. An approach for arsenic in a contaminated soil: speciation, fractionation, extraction and effluent decontamination. Environ. Pollut. 158, 416–423. https://doi.org/10.1016/j.envpol.2009.08.010.

Hakanson, L., 1980. An ecological risk index for aquatic pollution control. A sedimentological approach. Water Res. 14, 975–1001. https://doi.org/10.1016/0043-1354(80)90143-8.

Hinton, J.H., Veiga, M.M., 2009. Using earthworms to assess Hg distribution and bioavailability in gold mining soils. Soil Sediment Contam. 18, 512–524. https://doi.org/10.1080/15320380902978847.

Hu, X., Zhang, Y., Ding, Z., Wang, T., Lian, H., Sun, Y., Wu, J., 2012. Bioaccessibility and health risk of arsenic and heavy metals (Cd, Co, Cr, Cu, Ni, Pb, Zn and Mn) in TSP and PM2.5 in Nanjing, China. Atmos. Environ. Times 57, 146–152. https://doi.org/10.1016/j.atmosenv.2012.04.056.

Huang, X., Betha, R., Tan, L.Y., Balasubramanian, R., 2016. Risk assessment of bioaccessible trace elements in smoke haze aerosols versus urban aerosols using simulated lung fluids. Atmos. Environ. 125, 505–511. https://doi.org/10.1016/j.atmosenv.2015.06.034.

IBGE, 2018. IBGE Cidades - Cachoeira Do Piriá. Instituto Brasileiro de Geografia e Estatística.

INMET, 2018. Cachoeira Do Piriá - Pará: Clima. Brasília.

Izquierdo, M., Miguel, E., Ortega, M.F., Mingot, J., 2015. Bioaccessibility of metals and human health risk assessment in community urban gardens. Chemosphere 135, 312–318. https://doi.org/10.1016/j.chemosphere.2015.04.079.

Jiang, X., Zou, B., Feng, H., Tang, J., Tu, Y., Zhao, X., 2019. Spatial distribution mapping of Hg contamination in subclass agricultural soils using GIS enhanced multiple linear regression. J. Geochem. Explor. 196, 1–7. https://doi.org/10.1016/j.gexplo.2018.10.002.

Juhasz, A.L., Herde, P., Herde, C., Boland, J., Smith, E., 2014. Validation of the predictive capabilities of the Sbrc-G in vitro assay for estimating arsenic relative bioavailability in contaminated soils. Environ. Sci. Technol. 48, 12962–12969.

Juhasz, A.L., Weber, J., Smith, E., 2011. Influence of saliva, gastric and intestinal phases on the prediction of as relative bioavailability using the Unified Bioaccessibility Research Group of Europe Method (UBM). J. Hazard Mater. 197, 161–168. https://doi.org/10.1016/j.jhazmat.2011.09.068.

Kabata-Pendias, A., 2010. Trace elements in soils and plants. In: Trace Elements in Soils and Plants, fourth ed. CRC Press. https://doi.org/10.1201/b10158.

Kim, E.J., Yoo, J.-C., Baek, K., 2014. Arsenic speciation and bioaccessibility in arsenic-contaminated soils: sequential extraction and mineralogical investigation. Environ. Pollut. 186, 29–35. https://doi.org/10.1016/j.envpol.2013.11.032.

Kim, J.Y., Kim, K.W., Lee, J.U., Lee, J.S., Cook, J., 2002. Assessment of as and heavy metal contamination in the vicinity of Duckum Au-Ag mine, Korea. Environ. Geochem. Health 24, 215–227. https://doi.org/10.1023/A.

Klein, E.L., Lopes, E.C.S., Tavares, F.M., Campos, L.D., Souza-Gaia, S.M., Neves, M.P., Perrotta, M.M., 2017. Áreas de relevante interesse mineral Cinturão Gurupi - Estados do Pará e Maranhão (Brasília).

Kowalska, J.B., Mazurek, R., Gasiorek, M., Zaleski, T., 2018. Pollution indices as useful tools for the comprehensive evaluation of the degree of soil contamination - a review. Environ. Geochem. Health 40, 2395–2420. https://doi.org/10.1007/s10653-018-0106-z.

Kyle, J.H., Breuer, P.L., Bunney, K.G., Pleysier, R., 2012. Hydrometallurgy review of trace toxic elements (Pb, Cd, Hg, As, Sb, Bi, Se, Te) and their deportment in gold processing. Hydrometallurgy 111–112, 10–21. https://doi.org/10.1016/j.hydromet.2011.09.005.

Li, J., Wei, Y., Zhao, L., Zhang, J., Shangguan, Y., Li, F., Hou, H., 2014. Bioaccessibility of antimony and arsenic in highly polluted soils of the mine area and health risk assessment associated with oral ingestion exposure. Ecotoxicol. Environ. Saf. 110, 308–315. https://doi.org/10.1016/j.ecoenv.2014.09.009.

Li, S.W., Li, J., Li, H.B., Naidu, R., Ma, L.Q., 2015. Arsenic bioaccessibility in contaminated soils: coupling in vitro assays with sequential and HNO3 extraction. J. Hazard Mater. 295, 145–152. https://doi.org/10.1016/j.jhazmat.2015.04.011.

Lima, A., Vivo, B., Cicchella, D., Cortini, M., Albanese, S., 2003. Multifractal IDW interpolation and fractal filtering method in environmental studies: an application on regional stream sediments of (Italy), Campania region. Appl. Geochem. 18, 1853–1865. https://doi.org/10.1016/S0883-2927(03)00083-0.

Lin, W., Wu, K., Lao, Z., Hu, W., Lin, B., Li, Y., Fan, H., Hu, J., 2019. Assessment of trace metal contamination and ecological risk in the forest ecosystem of dexing mining area in northeast Jiangxi Province, China. Ecotoxicol. Environ. Saf. 167, 76–82. https://doi.org/10.1016/j.ecoenv.2018.10.001.

Lindsay, M.B.J., Moncur, M.C., Bain, J.G., Jambor, J.L., Ptacek, C.J., Blowes, D.W., 2015. Geochemical and mineralogical aspects of sulfide mine tailings. Appl. Geochem. 57, 157–177. https://doi.org/10.1016/j.apgeochem.2015.01.009.

Liu, X., Song, Q., Tang, Y., Li, W., Xu, J., Wu, J., Wang, F., Charles, P., 2013. Human health risk assessment of heavy metals in soil-vegetable system: a multimedium analysis. Sci. Total Environ. 463–464, 530–540. https://doi.org/10.1016/j.scitotenv.2013.06.064.

Lu, X., Zhang, X., Li, L.Y., Chen, H., 2014. Assessment of metals pollution and health risk in dust from nursery schools in Xi'an, China. Environ. Res. 128, 27–34. https://doi.org/10.1016/j.envres.2013.11.007.

Martinez-lladó, X., Vilà, M., Martí, V., Rovira, M., Domènech, J.A., Pablo, J., 2008. Trace element distribution in topsoils in Catalonia: background and reference values and relationship with regional geology. Environ. Eng. Sci. 25, 863–878. https://doi.org/10.1089/ees.2007.0139.

Matos, C.H.L., Melo, V.F., Pereira, S.C., Nascimento, P.P.R.R., Pereira, R.A., 2017. Phosphorus adsorption in soils under forest and savanna from Northern Amazon, Brazil. Semin. Ciências Agrárias 38, 2909–2920. https://doi.org/10.5433/1679-0359.2017v38n5p2909.

McGrath, S.P., Cunliffe, C.H., 1985. A simplified method for the extraction of the metals Fe, Zn, Cu, Ni, Cd, Pb, Cr, Co and Mn from soils and sewage sludges. J. Sci. Food Agric. 36, 794–798.

Melo, G.H.C., Monteiro, L.V.S., Moreto, C.P.N., Xavier, R.P., Silva, M.A.D., 2014. Paragenesis and evolution of the hydrothermal Bacuri iron oxide-copper-gold deposit, Carajás Province (PA). Brazil. J. Geol. 44, 73–90. https://doi.org/10.5327/Z2317-4889201400010007.

Mendoza, C.J., Garrido, R.T., Quilodrán, R.C., Segovia, C.M., Parada, A.J., 2017. Evaluation of the bioaccessible gastric and intestinal fractions of heavy metals in contaminated soils by means of a simple bioaccessibility extraction test. Chemosphere 176, 81–88. https://doi.org/10.1016/j.chemosphere.2017.02.066.

Mensah, A.K., Marschner, B., Shaheen, S.M., Wang, J., Wang, S.-L., Rinklebe, J., 2020. Arsenic contamination in abandoned and active gold mine spoils in Ghana: geochemical fractionation, speciation, and assessment of the potential human health risk. Environ. Pollut. 261, 114116. https://doi.org/10.1016/j.envpol.2020.114116.

Minatel, B.C., Sage, A.P., Anderson, C., Hubaux, R., Marshall, E.A., Lam, W.L., Martinez, V.D., 2018. Environmental arsenic exposure: from genetic susceptibility to pathogenesis. Environ. Int. 112, 183–197. https://doi.org/10.1016/j.envint.2017.12.017.

MMA, 2001. Manual de normas e procedimentos para licenciamento ambiental no setor de extração mineral. Brasília.

Moreira, L.J.D., Silva, E.B., Fontes, M.P.F., Liu, X., Ma, L.Q., 2018. Speciation, bioaccessibility and potential risk of chromium in Amazon forest soils. Environ. Pollut. 239, 384–391. https://doi.org/10.1016/j.envpol.2018.04.025.

Mosher, G.Z., 2013. Technical Report and Resource Estimate on the Cachoeira Property. Pará state, Brazil. Vancouver.

Murciego, A., Álvarez-Ayuso, E., Pellitero, E., Rodríguez, M.A., García-Sánchez, A., Tamayo, A., Rubio, F., Rubin, J., 2011. Study of arsenopyrite weathering products in mine wastes from abandoned tungsten and tin exploitations. J. Hazard Mater. J. 186, 590–601. https://doi.org/10.1016/j.jhazmat.2010.11.033.

Ngole-Jeme, V.M., Fantke, P., 2017. Ecological and human health risks associated with abandoned gold mine tailings contaminated soil. PloS One 12, e0172517. https://doi.org/10.1371/journal.pone.0172517.

Odumo, B.O., Nanos, N., Carbonell, G., Torrijos, M., Patel, J.P., Rodríguez Martín, J.A., 2018. Artisanal gold-mining in a rural environment: land degradation in Kenya. Land Degrad. Dev. 29, 3285–3293. https://doi.org/10.1002/ldr.3078.

Ono, F.B., Guilherme, L.R.G., Penido, E.S., Carvalho, G.S., Hale, B., Toujaguez, R., Bundschuh, J., 2012. Arsenic bioaccessibility in a gold mining area: a health risk assessment for children. Environ. Geochem. Health 34, 457–465. https://doi.org/10.1007/s10653-011-9444-9.

Ono, F.B., Tappero, R., Sparks, D., Guilherme, L.R.G., 2015. Investigation of arsenic species in tailings and windblown dust from a gold mining area. Environ. Sci. Pollut. Res. 23, 638–647. https://doi.org/10.1007/s11356-015-5304-y.

Park, J.H., Choi, K.K., 2013. Risk assessment of soil, water and crops in abandoned Geumryeong mine in South Korea. J. Geochem. Explor. 128, 117–123. https://doi.org/10.1016/j.gexplo.2013.02.004.

Pereira, W.V. da S., Teixeira, R.A., Souza, E.S. de, Moraes, A.L.F. de, Campos, W.E.O., Amarante, C.B. do, Martins, G.C., Fernandes, A.R., 2020. Chemical fractionation and bioaccessibility of potentially toxic elements in area of artisanal gold mining in the Amazon. J. Environ. Manag. 267, 110644. https://doi.org/10.1016/j.jenvman.2020.110644.

Pérez-Moreno, S.M., Gázquez, M.J., Pérez-López, R., Bolivar, J.P., 2018. Validation of the BCR sequential extraction procedure for natural radionuclides. Chemosphere 198, 397–408. https://doi.org/10.1016/j.chemosphere.2018.01.108.

R Core Team, 2017. R: A Language and Environment for Statistical Computing.

Ramirez-andreotta, M.D., Brusseau, M.L., Beamer, P., Maier, R.M., 2013. Home gardening near a mining site in an arsenic-endemic region of Arizona: assessing arsenic exposure dose and risk via ingestion of home garden vegetables, soils, and water. Sci. Total Environ. 454–455, 373–382. https://doi.org/10.1016/j.scitotenv.2013.02.063.

Ribeiro, J.W.A., 2002. O arcabouço estrutural da região de Chega Tudo e Cedral, NW do Maranhão, com base em sensores geofisicos. Universidade Federal do Pará.

Rieuwerts, J.S., Mighanetara, K., Braungardt, C.B., Rollinson, G.K., Pirrie, D., Azizi, F., 2014. Geochemistry and mineralogy of arsenic in mine wastes and stream sediments in a historic metal mining area in the UK. Sci. Total Environ. 472, 226–234. https://doi.org/10.1016/j.scitotenv.2013.11.029.

Sah, D., Verma, P.K., Kumari, K.M., Lakhani, A., 2019. Chemical fractionation of heavy metals in fine particulate matter and their health risk assessment through inhalation exposure pathway. Environ. Geochem. Health 41, 1445–1458. https://doi.org/10.1007/s10653-018-0223-8.

Santos, R.N. do E.S., 2004. Investigação do passivo ambiental em Cachoeira do Piriá, NE do Pará: base para a gestão ambiental em áreas garimpadas na Amazônia. Universidade de São Paulo.

Shaheen, S.M., Kwon, E.E., Biswas, J.K., Tack, F.M.G., Ok, Y.S., Rinklebe, J., 2017. Arsenic, chromium, molybdenum, and selenium: geochemical fractions and potential mobilization in riverine soil profiles originating from Germany and Egypt. Chemosphere 180, 553–563. https://doi.org/10.1016/j.chemosphere.2017.04.054.

Sheik, C.S., Mitchell, T.W., Rizvi, F.Z., Rehman, Y., Faisal, M., Hasnain, S., McInerney, M.J., Krumholz, L.R., 2012. Exposure of soil microbial communities to chromium and arsenic alters their diversity and structure. PloS One 7, e40059. https://doi.org/10.1371/journal.pone.0040059.

Souza, E.S., Fernandes, A.R., Braz, A.M. de S., Sabino, L.L.L., Alleoni, L.R.F., 2015. Potentially toxic elements (PTEs) in soils from the surroundings of the Trans-Amazonian Highway, Brazil. Environ. Monit. Assess. 187, 4074. https://doi.org/10.1007/s10661-014-4074-1.

Souza, E.S., Texeira, R.A., Costa, H.S.C., Oliveira, F.J., Melo, L.C.A., Faial, K.C.F., Fernandes, A.R., 2017. Assessment of risk to human health from simultaneous exposure to multiple contaminants in an artisanal gold mine in Serra Pelada, Pará, Brazil. Sci. Total Environ. 576, 683–695. https://doi.org/10.1016/j.scitotenv.2016.10.133.

Sun, Y., Hu, X., Wu, J., Lian, H., Chen, Y., 2014. Fractionation and health risks of atmospheric particle-bound as and heavy metals in summer and winter. Sci. Total Environ. 493, 487–494. https://doi.org/10.1016/j.scitotenv.2014.06.017.

Tapia-Gatica, J., González-Miranda, I., Salgado, E., Bravo, M.A., Tessini, C., Dovletyarova, E.A., Paltseva, A.A., Neaman, A., 2020. Advanced determination of the spatial gradient of human health risk and ecological risk from exposure to As, Cu, Pb, and Zn in soils near the Ventanas Industrial Complex (Puchuncaví, Chile). Environ. Pollut. 258, 113488. https://doi.org/10.1016/j.envpol.2019.113488.

Teixeira, P.C., Donagemma, G.K., Fontana, A., Teixeira, W.G. (Eds.), 2017a. Manual de métodos de análise de solo, third ed. Embrapa Solos, Brasília.

Teixeira, R.A., Fernandes, A.R., Ferreira, J.R., Vasconcelos, S.S., Braz, A.M. de S., 2018. Contamination and soil biological properties in the Serra Pelada mine - amazônia, Brazil. Rev. Bras. Ciência do Solo 42, 1–15. https://doi.org/10.1590/18069657rbcs20160354.

Teixeira, R.A., Souza, E.S., Fernandes, A.R., 2017b. Elementos potencialmente tóxicos e índices de poluição em solos e sedimentos do garimpo de Serra Pelada. Brasil. Cienc. del suelo 35, 377–384.

Teixeira, R.A., Souza, E.S., Lima, M.W., Dias, Y.N., Pereira, W.V. da S., Fernandes, A.R., 2019. Index of geoaccumulation and spatial distribution of potentially toxic elements in the Serra Pelada gold mine. J. Soils Sediments 19, 2934–2945. https://doi.org/10.1007/s11368-019-02257-y.

Thouin, H., Battaglia-Brunet, F., Norini, M.-P., Forestier, L.L., Charron, M., Dupraz, S., Gautret, P., 2018. Influence of environmental changes on the biogeochemistry of arsenic in a soil polluted by the destruction of chemical weapons: a mesocosm study. Sci. Total Environ. 627, 216–226. https://doi.org/10.1016/j.scitotenv.2018.01.158.

USEPA, 2001. Supplemental Guidance for Developing Soil Screening Levels for Superfund Sites. Office of Solid Waste and Emergency Response, Washington.

Venegas, V.H.A., Novais, R.F., Barros, N.F., Cantarutti, R.B., Lopes, A.S., 1999. Interpretation of soil analysis results. In: Recommendations for the Use of Correctives and Fertilizers in Minas Gerais. Comissão de Fertilidade do Solo do Estado de Minas Gerais, Viçosa, pp. 25–32.

Wang, S., Mulligan, C.N., 2006. Occurrence of arsenic contamination in Canada: sources, behavior and distribution. Sci. Total Environ. 366, 701–721. https://doi.org/10.1016/j.scitotenv.2005.09.005.

Wragg, J., Cave, M., Basta, N., Brandon, E., Casteel, S., Denys, S., Gron, C., Oomen, A., Reimer, K., Tack, K., Wiele, T.V., 2011. An inter-laboratory trial of the unified BARGE bioaccessibility method for arsenic, cadmium and lead in soil. Sci. Total Environ. 409, 4016–4030. https://doi.org/10.1016/j.scitotenv.2011.05.019.

Xiao, R., Guo, D., Ali, A., Mi, S., Liu, T., Ren, C., Li, R., Zhang, Z., 2019. Accumulation, ecological-health risks assessment, and source apportionment of heavy metals in paddy soils: a case study in Hanzhong, Shaanxi, China. Environ. Pollut. 248, 349–357. https://doi.org/10.1016/j.envpol.2019.02.045.

Yusà, V., Pérez, R., Sánchez, A., Pardo, O., Roca, M., 2018. Exposure and risk assessment to arsenic species in Spanish children using biomonitoring. Sci. Total Environ. 628–629, 302–309. https://doi.org/10.1016/j.scitotenv.2018.01.330.

Zhang, P., Qin, C., Hong, X., Kang, G., Qin, M., Yang, D., Pang, B., Li, Y., He, J., Dick, R.P., 2018. Risk assessment and source analysis of soil heavy metal pollution from lower reaches of Yellow River irrigation in China. Sci. Total Environ. 633, 1136–1147. https://doi.org/10.1016/j.scitotenv.2018.03.228.

Zhou, Q., Teng, Y., Liu, Y., 2017. A study on soil-environmental quality criteria and standards of arsenic. Appl. Geochem. 77, 158–166. https://doi.org/10.1016/j.apgeochem.2016.05.001.

Zvarivadza, T., 2018. Artisanal and small-scale mining as a challenge and possible contributor to sustainable development. Resour. Pol. 56, 49–58. https://doi.org/10.1016/j.resourpol.2018.01.009.